Plant Physiol. (1989) 91, 352–356
0032-0889/89/91/0352/05/$01.00/0

Received for publication January 24, 1989
and in revised form May 8, 1989

# Oxygen and Carbon Dioxide Fluxes from Barley Shoots Depend on Nitrate Assimilation[1]

**Arnold J. Bloom*, Richard M. Caldwell, John Finazzo, Robert L. Warner, and Joseph Weissbart**

*Department of Vegetable Crops, University of California, Davis, California 95616* (A.J.B., R.M.C., J.F.); *Agronomy and Soils Department, Washington State University, Pullman Washington 99164* (R.L.W.); *and Bart Medical Company, Los Gatos, California 95030* (J.W.)

## ABSTRACT

**A custom oxygen analyzer in conjunction with an infrared carbon dioxide analyzer and humidity sensors permitted simultaneous measurements of oxygen, carbon dioxide, and water vapor fluxes from the shoots of intact barley plants (*Hordeum vulgare* L. cv Steptoe). The oxygen analyzer is based on a calcia-zirconium sensor and can resolve concentration differences to within 2 microliters per liter against the normal background of 210,000 microliters per liter. In wild-type plants receiving ammonium as their sole nitrogen source or in nitrate reductase-deficient mutants, photosynthetic and respiratory fluxes of oxygen equaled those of carbon dioxide. By contrast, wild-type plants exposed to nitrate had unequal oxygen and carbon dioxide fluxes: oxygen evolution at high light exceeded carbon dioxide consumption by 26% and carbon dioxide evolution in the dark exceeded oxygen consumption by 25%. These results indicate that a substantial portion of photosynthetic electron transport or respiration generates reductant for nitrate assimilation rather than for carbon fixation or mitochondrial electron transport.**

The influence of $NO_3^-$ assimilation upon photosynthesis and respiration has been the subject of much speculation (9, 17, 20, 25). To provide energy for $NO_3^-$ assimilation, a portion of the electrons that are usually transferred to $CO_2$ during photosynthesis or to $O_2$ during respiration may be instead transferred to $NO_3^-$ and $NO_2^-$ (1, 19). Thus, under $NO_3^-$ nutrition, the light reactions of photosynthesis should evolve $O_2$ faster than carbon fixation consumes $CO_2$ ( *i.e.* the AQ[2] should decrease) or carbohydrate catabolism should evolve $CO_2$ faster than mitochondrial electron transport consumes $O_2$ (*i.e.* the RQ should increase). These phenomena have previously been examined only in algae. For *Chlorella*, a change from $NH_4^+$ to $NO_3^-$ nutrition shifted the AQ from 0.94 to 0.68 and the RQ from 1.2 to 1.6 (18); for *Selenastrum minutum*, the RQ shifted from 0.84 to 8.13 (29).

There are relatively few estimates of AQ or RQ in higher plants. This stems primarily from difficulties in measuring $O_2$ and $CO_2$ fluxes concurrently. When monitoring shoot gas fluxes, the relative depletion of $CO_2$ must be kept small to avoid significant changes in the rate of carbon fixation. Small depletions in $CO_2$ concentration are associated with minuscule increases in $O_2$ concentration because the normal background levels of $CO_2$ and $O_2$ are 350 and 209,460 $\mu$L $L^{-1}$, respectively. For example, experimental conditions that deplete $CO_2$ by 10% would increase $O_2$ by less than 0.02%.

Several approaches have been employed to monitor oxygen fluxes from plants, but each has serious disadvantages: (a) micromanometric techniques require that the organism be enclosed in a tightly-sealed, highly temperature-controlled chamber (12); consequently, these techniques have not been amenable to studies of intact plants. (b) Mass spectrometric analysis can provide simultaneous estimates of oxygen production and uptake (8, 26). Plant material is exposed to an atmosphere highly enriched with the heavy isotope $^{18}O$. Changes in the levels of $^{16}O$ and $^{18}O$ indicate rates of oxygen production and uptake, respectively. These systems cannot monitor water fluxes and, therefore, cannot estimate intercellular $CO_2$ concentrations. (c) Paramagnetic analyzers can resolve small $O_2$ concentration differences (11), but demonstrate a high sensitivity to gas flow rate and vibration (16). (d) The signal drift and noise of polarographic $O_2$ sensors require that relatively large ($\approx$300 $\mu$L $L^{-1}$) $O_2$ depletions be obtained (13, 14). (e) Commercial instruments based on ceramic electrolytic cells have had adequate sensitivity and stability only at very low ambient $O_2$ concentrations ($\approx$2000 $\mu$L $L^{-1}$) (4, 15).

Here we describe an oxygen analyzer based on a ceramic electrolytic cell that has sufficient resolution to monitor plant $O_2$ fluxes at normal $O_2$ levels. We have used this instrument to study the influence of $NO_3^-$ assimilation on shoot photosynthesis and respiration.

## MATERIALS AND METHODS

### Oxygen Analyzer Design

The differential $O_2$ analyzer contains two cells of a calcia-stabilized zirconium oxide ceramic similar to those found in an Applied Electrochemistry model N-37M sensor. Each cell is in the shape of a cylinder with a flat, closed end; the closed end has platinum electrodes inside and out. The two cells are arranged within an electric furnace so that their closed ends are parallel to one another about 2 mm apart. Sample gases flow through the inside of each cell; the outsides of the cells are in contact with a reference gas. At elevated temperatures, the ceramic becomes selectively permeable to $O_2$ and each

[1] Supported in part by National Science Foundation Grants BSR-84-16893 and BSR-88-06585 and USDA Grant 88-37264-3857.

[2] Abbreviations: AQ, assimilatory quotient; NR, nitrate reductase; RQ, respiratory quotient.

cell generates an electrical potential dependent on the difference in $O_2$ partial pressures across the ceramic according to:

$$E = \frac{RT}{nF} ln \frac{P_r}{P_s} \quad (1)$$

where $R$ is the gas constant (8.314 joule $mol^{-1}$ $K^{-1}$); $T$ is the cell temperature in $K$; $n$ is the number of equivalents per unit electrode reaction (4 for this electrode); $F$ is Faraday's constant (96,500 coulombs $mol^{-1}$); $P_r$ is the partial pressure of $O_2$ in the reference gas; and $P_s$ is the partial pressure of $O_2$ in the sample gas (30). At an operating temperature of 752°C and a background $O_2$ level of 209,460 $\mu$L $L^{-1}$, this equation predicts a 106 nV potential difference between the cells per $\mu$L $L^{-1}$ difference in $O_2$ partial pressures.

To measure potential differences on the order of 106 nV requires a high quality amplifier. The amplifier developed for this instrument has 20 nV peak to peak noise with a bandwidth of 1 Hz and 20 nV $week^{-1}$ and 8 nV $°C^{-1}$ zero offset drift. Its power requirements are ±15 V at 8 ma. This amplifier should prove useful for other applications needing amplification of very small signals such as thermocouple psychrometry.

The output of each cell is temperature dependent (≈50 $\mu$V $°C^{-1}$; Eq. 1); thus, to achieve a zero stability of better than 2 $\mu$L $L^{-1}$, the temperature difference between cells must not fluctuate more than 0.004°C. A platinum resistance temperature detector (RTD) is situated near the center of the furnace. This RTD forms one leg of a Wheatstone bridge designed to balance when the RTD reaches a temperature 752°C. The signal from the bridge drives a proportional, integrative, and derivative controller that regulates power to the furnace. This arrangement holds the temperature to within the required limits.

Cell potential also varies with the rate of gas flowing through it, presumably because the flow affects cell temperature. A dual-headed, gas metering pump (Fluid Metering Inc.) maintains the same flow through both cells (Fig. 1).

Water vapor interferes with $O_2$ or $CO_2$ measurements. The partial pressure of water vapor in a sample dilutes the partial pressures of $O_2$ and $CO_2$. Moreover, water and $CO_2$ absorb infrared energy at some of the same wavelengths. In this system, water vapor pressure in the gas samples is decreased to a constant, low level by a stainless-steel condensor cooled to 5°C with Peltier thermoelectric devices (Fig. 1). This avoids the use of desiccants that can produce significant measurement artifacts (23).

### Analyzer Calibration

Calibration of the $O_2$ analyzer requires standard gases that differ by a tiny, precise amount. To produce such standards: (a) pure $N_2$ in a compressed gas cylinder was released until the cylinder pressure reached equilibrium with the atmosphere. (b) This cylinder, $C_1$, was filled with half the contents of a compressed air cylinder, $C_2$; thus, the first cylinder $C_1$ contained approximately 7.5 MPa of air diluted by 0.1 MPa of $N_2$. (c) The $O_2$ concentrations of both cylinders, $C_1$ and $C_2$, were determined with the $O_2$ analyzer serving as a null detector: (i) a zero reading was obtained by flowing the gas from $C_1$ or $C_2$ through both cells of the analyzer; (ii) known concentrations of $O_2$ were generated by mixing pure $O_2$ and $N_2$ with mass flow controllers (Tylan) which had been calibrated against a soap-bubble flowmeter; (iii) the gas from $C_1$ or $C_2$ flowed through one cell and various concentrations of $O_2$ flowed through the other cell until the analyzer indicated the zero reading. The $O_2$ concentrations in $C_1$ and $C_2$ usually differed by about 2,800 $\mu$L $L^{-1}$. (d) With the gas from $C_1$ flowing through one cell of the analyzer and a mixture of $C_1$ and $C_2$ generated by the mass flow controllers flowing through the other cell, $O_2$ concentration differences of 28 to 2,800 $\mu$L $L^{-1}$ could accurately be generated on a background of 209,460 $\mu$L $L^{-1}$.

### Analyzer Performance

The $O_2$ analyzer exhibited a noise level of 100 nV ($V_{rms}$), a drift of less than 200 nV $h^{-1}$, a response time of less than 1 min, and a linear response ($R^2$ = 0.999) of 109 nV per $\mu$L $L^{-1}$ differential in $O_2$ when air containing 20.890% $O_2$ flowed through one cell and air containing 20.900 to 20.915% $O_2$ flowed through the other (Fig. 2). Calibrations conducted several weeks apart obtained the same slope.

### Plant Material and Methods

We used a wild-type barley cultivar (*Hordeum vulgare* L. cv Steptoe) and a double mutant (*nar*1a;*nar*7w) that is deficient in both NADH and NAD(P)H nitrate reductases (28). These genotypes were germinated on wet toweling and then suspended above light-tight root boxes containing 4 L of a dilute Hoagland nutrient solution similar to that used previously (6) except that 75 $\mu$M $NH_4H_2PO_4$ was the sole nitrogen source. This solution was replenished every other day. The seedlings were grown in a temperature-controlled greenhouse at 25°C. Supplemental lighting kept the photon flux at plant height greater than 1000 $\mu$mol photons $m^{-2}$ $s^{-1}$ during the 14-h light period.

About 2 weeks after germination, when the third leaf was emerging, a plant was exposed for 24 h to a nutrient solution containing either 50 $\mu$M $NH_4H_2PO_4$ or 50 $\mu$M $KNO_3$. This plant was then transferred to a measurement system in which the roots and the shoot were enclosed by separate, but contiguous, cuvettes (24). To allow for recovery from any transplant shock, the plant was maintained in the dark for at least 8 h before experimental data were taken. A nutrient solution containing either 50 $\mu$M $NH_4Cl$ or 50 $\mu$M $KNO_3$ as the nitrogen source flowed continuously through the root cuvette. The roots were kept in the dark at 15°C while the shoot was kept at a leaf temperature of 25°C and a vapor pressure deficit of about 0.5 Pa.

Root $NO_3^-$ absorption was calculated from the depletion of $NO_3^-$ as the nutrient solution passed through the root cuvette (5). Plant $NO_3^-$ assimilation was taken as the difference between the total amount of $NO_3^-$ absorbed from the medium and the total $NO_3^-$ accumulated in the root and shoot as determined by ion chromatography (3). Shoot fluxes were monitored using an open gas-exchange system (Fig. 1) (24). An infrared gas analyzer (Horiba VIA-500R) and humidity sensors (Vaisala) measured net fluxes of $CO_2$ and $H_2O$, respectively. Intercellular $CO_2$ concentration was estimated

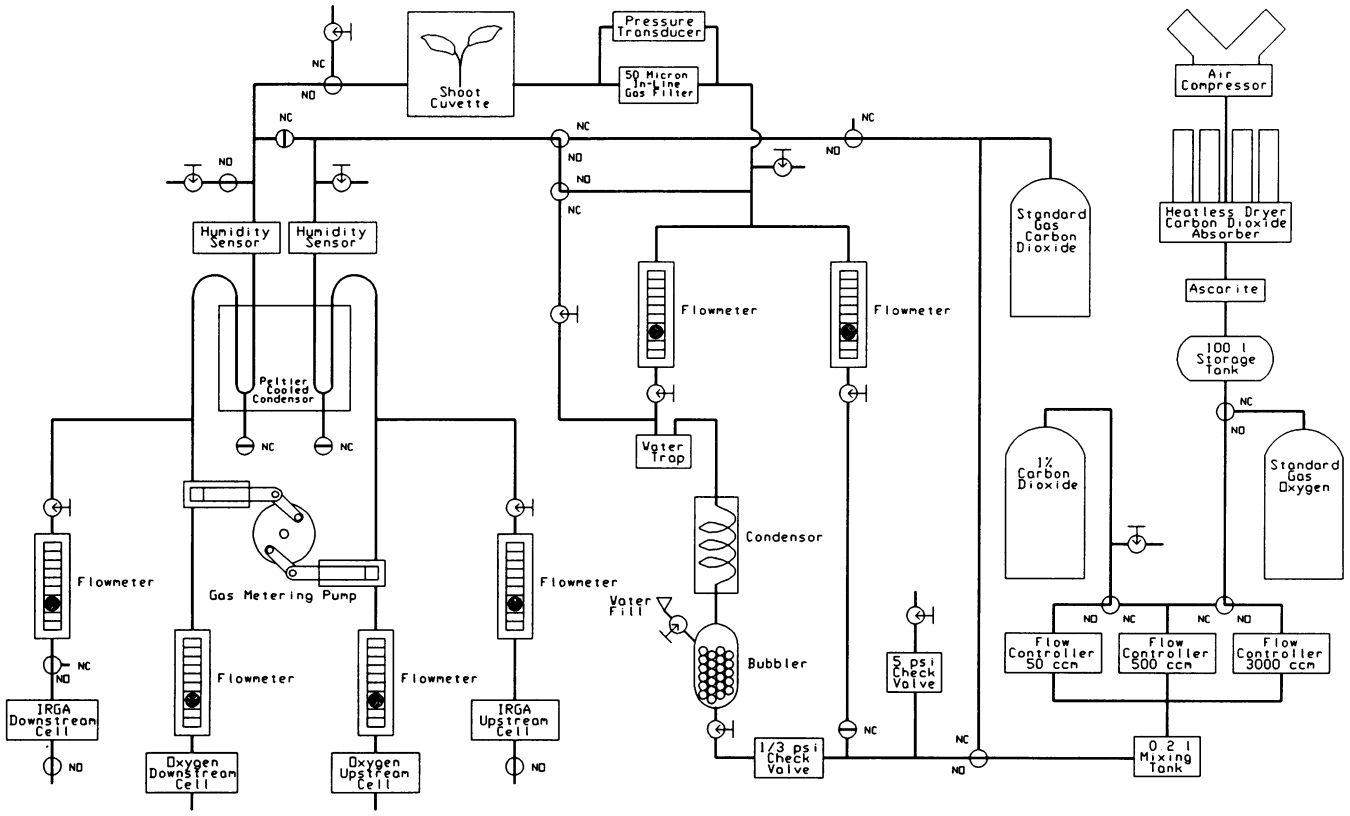


**Figure 1.** Block diagram of the open gas-exchange system used to monitor shoot fluxes of $O_2$, $CO_2$, and $H_2O$: solenoid valves are represented by circles with the normally open and closed directions indicated by NO and NC, respectively; manual valves are represented by circles with stems; other parts are labeled.

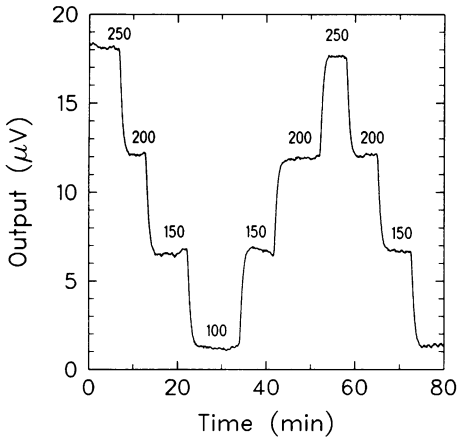


**Figure 2.** Chart recorder tracing of the output from the $O_2$ analyzer showing its response when air containing 208,900 $\mu$L $L^{-1}$ $O_2$ flowed through one cell and air containing a concentration higher by 100, 150, 200, or 250 $\mu$L $L^{-1}$ $O_2$ flowed through the other.

from the external concentration and the diffusion resistance for water vapor exchange (27). The experimental protocols for evaluating the response of photosynthesis to changes in $CO_2$ concentration or light level followed those described previously (7). To compare assimilatory and respiratory quotients of the wild type with those of the mutant, plants were monitored in the dark for about 4 h and then at a light level of 1200 $\mu$mol photons $m^{-2}$ $s^{-1}$ for about 4 h.

## RESULTS AND DISCUSSION

Under most conditions, net $O_2$ and $CO_2$ fluxes were equal (Table I; Figs. 3 and 4). Only the wild type exposed to $NO_3^-$—plants that were assimilating significant amounts of $NO_3^-$—had assimilatory or respiratory quotients that deviated from unity (Table I). Those plants evolved more $O_2$ at high light levels than they consumed $CO_2$ (Fig. 4B); presumably, either the light reactions of photosynthesis proceeded faster than the dark reactions or carbohydrate catabolism proceeded faster than mitochondrial electron transport. Also, net $O_2$ consumption by the wild type did not keep pace with net $CO_2$ evolution after 4 h in the dark (Table I), probably because mitochondrial electron transport was slower than carbohydrate catabolism. These results suggest that significant portions of photosynthetic electron transport and mitochondrial respiration (26 and 25%, respectively; Table I; Fig. 4), were coupled to $NO_3^-$ assimilation.

Nitrate assimilation did not appear competitive with carbon fixation. Rates of net $CO_2$ consumption were similar among both the $NH_4^+$- and $NO_3^-$-treated plants at all intercellular $CO_2$ concentrations and light levels (Figs. 3 and 4). Only at high light levels and normal $CO_2$ concentrations did net $O_2$ evolution exceed net $CO_2$ consumption (Fig. 4). Availability of $CO_2$, not availability of reductant, probably limited carbon fixation under these conditions (27); thus, diversion of reductant to $NO_3^-$ assimilation should not diminish carbon fixation.

**Table I.** *Shoot $CO_2$ and $O_2$ Fluxes, Respiratory and Assimilatory Quotients, Root $NO_3^-$ Absorption, and Plant $NO_3^-$ Assimilation by Intact Barley Plants*

Gas fluxes are per unit area shoot (mean ± SE, $n = 8$); $NO_3^-$ absorption is per unit dry weight root (mean ± SE, $n = 8$); $NO_3^-$ assimilation is per unit dry weight plant (mean ± SE, $n = 6$). The respiratory quotient, RQ, and the assimilatory quotient, AQ, that are given are the means ± SE ($n = 8$) of the ratios, not the ratio of the means. 'WT' indicates the wild-type *Hordeum vulgare* L. cv Steptoe and *nar*1a;*nar*7w indicates a mutant of this cultivar that is deficient in NADH and NAD(P)H nitrate reductases. Root $NO_3^-$ absorption was calculated from the depletion of $NO_3^-$ as the nutrient solution passed through the root cuvette. Plant $NO_3^-$ assimilation was determined from the difference between the total amount of $NO_3^-$ that the plant absorbed and the total amount of $NO_3^-$ that accumulated in the root and shoot. The gas entering the shoot cuvette contained 380 $\mu$L $L^{-1}$ $CO_2$ and 208,000 $\mu$L $L^{-1}$ $O_2$. The light level for the Light treatment was 1200 $\mu$mol photons $m^{-2}$ $s^{-1}$.

| Genotype | Dark | | | | | Light | | | | |
|---|---|---|---|---|---|---|---|---|---|---|
| | $CO_2$ release | $O_2$ uptake | RQ | $NO_3^-$ uptake | $NO_3^-$ assimilation | $CO_2$ uptake | $O_2$ release | AQ | $NO_3^-$ uptake | $NO_3^-$ assimilation |
| | ($\mu$mol $m^{-2}$ $min^{-1}$) | ($\mu$mol $m^{-2}$ $min^{-1}$) | | ($\mu$mol $g^{-1}$ $min^{-1}$) | ($\mu$mol $g^{-1}$ $min^{-1}$) | ($\mu$mol $m^{-2}$ $min^{-1}$) | ($\mu$mol $m^{-2}$ $min^{-1}$) | | ($\mu$mol $g^{-1}$ $min^{-1}$) | ($\mu$mol $g^{-1}$ $min^{-1}$) |
| WT | 75.0 ± 7.2 | 55.2 ± 10.2 | 1.51 ± 0.13 | 0.49 ± 0.04 | 0.15 ± 0.01 | 562 ± 32 | 664 ± 48 | 0.86 ± 0.02 | 0.57 ± 0.06 | 0.17 ± 0.01 |
| *nar*1a;*nar*7w | 72.6 ± 9.0 | 76.8 ± 9.6 | 0.96 ± 0.07 | 0.64 ± 0.07 | 0.04 ± 0.01 | 346 ± 42 | 353 ± 43 | 0.98 ± 0.04 | 0.70 ± 0.09 | 0.03 ± 0.02 |

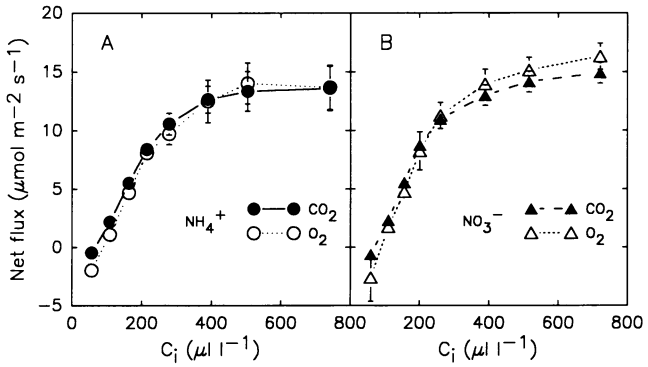


**Figure 3.** Influence of intercellular $CO_2$ concentration, $C_i$, on net $CO_2$ influx (closed symbols) and net $O_2$ efflux (open symbols) for Steptoe barley treated with $NH_4^+$ (Fig. 1A) or $NO_3^-$ (Fig. 1B). Shown are mean ± SE, $n = 3$, with small errors incorporated into the symbols.

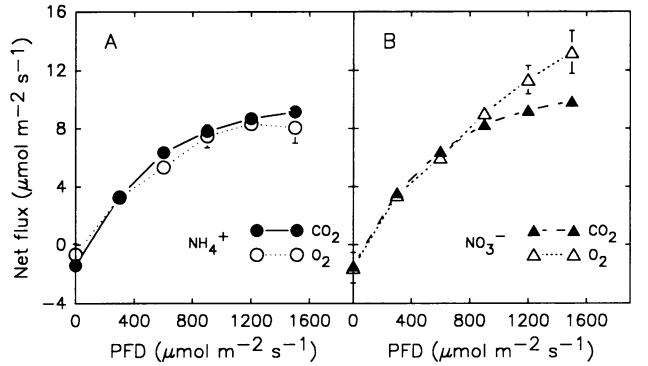


**Figure 4.** Influence of photosynthetic flux density, PFD, on net $CO_2$ influx (closed symbols) and net $O_2$ efflux (open symbols) for Steptoe barley treated with $NH_4^+$ (Fig. 1A) or $NO_3^-$ (Fig. 1B). Shown are mean ± SE, $n = 3$, with small errors incorporated into the symbols.

These data provide additional evidence that chloroplast electron transport has a capacity beyond that immediately required for carbon fixation. This surplus capacity not only serves $NO_2^-$ reduction (21, 22), but supplies reductant for $SO_4^{2-}$ assimilation (2) and prolongs carbon fixation after brief exposures to high light (15).

Surplus reductant might also be available for $NO_3^-$ assimilation when low intercellular $CO_2$ concentrations limit carbon fixation. We found, however, that the assimilatory quotients remained close to unity even near the $CO_2$ compensation point (Fig. 3). Conditions of low $CO_2$ and normal $O_2$ can stimulate photorespiration and other $O_2$ consuming processes(8); such processes could expend any surplus reductant or, at least, obscure detection of $NO_3^-$ assimilation on the basis of net $O_2$ evolution.

Net $CO_2$ evolution in the dark was uniform among all treatments and genotypes (Table I; Fig. 4). After 4 h in the dark, the wild type that was assimilating substantial amounts of $NO_3^-$ had less net $O_2$ consumption than the mutant (Table I). This suggests that $NO_3^-$ assimilation and mitochondrial electron transport compete directly for reductant and is consistent with observations that $NO_3^-$ reductase can efficiently trap NADH produced in the mitochondria (19).

The effects of $NO_3^-$ assimilation on $CO_2$ and $O_2$ fluxes from the alga *Selenastrum minutum* (10, 29) contrast sharply with those observed here. Dark $CO_2$ evolution doubled under $NO_3^-$ nutrition in *S. minutum* but did not change in barley. Dark $O_2$ consumption increased slightly in *S. minutum* but decreased in barley. Under saturating light levels, net $CO_2$ consumption became negative in *S. minutum* (gross consumption and release were 74 and 188 $\mu$mol $CO_2$ $mg^{-1}$ Chl $h^{-1}$, respectively) but did not change in barley; net $O_2$ evolution did not change in *S. minutum* but increased in barley. Apparently, the alga and the higher plant differ fundamentally in their partitioning of energy to $NO_3^-$ assimilation.

In summary, we compared a wild-type barley and a NR-deficient mutant under $NH_4^+$ and $NO_3^-$ nutrition to examine the interaction between $NO_3^-$ assimilation and photosynthesis or respiration. Significant amounts of photosynthesis or respiration appeared to be coupled to $NO_3^-$ assimilation. $NO_3^-$ assimilation appeared to have little effect upon carbon fixation in the light, but appeared to decrease mitochondrial electron transport in the dark. These results support speculation that the energy requirements of $NO_3^-$ assimilation should not influence plant growth in high light environments but may stunt growth under more light-limited conditions (9, 17, 20).

## LITERATURE CITED


1. **Abrol YB, Sawhney SK, Naik MS** (1983) Light and dark assimilation of nitrate in plants. Plant Cell Environ **6:** 595–599
2. **Anderson JW** (1980) Assimilation of inorganic sulfate into cysteine. *In* BJ Miflin, ed, The Biochemistry of Plants: Amino Acids and Derivatives, Vol 5. Academic Press, New York, pp 203–225
3. **Aslam M, Huffaker RC, Rains DW** (1984) Early effects of salinity on nitrate assimilation in barley seedlings. Plant Physiol **76:** 321–325
4. **Björkman O, Gauhl E** (1970) Use of the zirconium oxide ceramic cell for measurements of photosynthetic oxygen evolution by intact leaves. Photosynthetica **4:** 123–128
5. **Bloom AJ** (1989) Continuous and steady-state nutrient absorption by intact plants. *In* JG Torrey, LJ Winship, eds, Application of Continuous and Steady-State Methods to Root Biology. Kluwer Academic Publishers, Dordrecht, pp 147–163
6. **Bloom AJ, Caldwell RM** (1988) Root excision decreases nutrient absorption and gas fluxes. Plant Physiol **87:** 794–796
7. **Bloom AJ, Mooney HA, Björkman O, Berry J** (1980) Materials and methods for carbon dioxide and water exchange analysis. Plant Cell Environ **3:** 371–376
8. **Canvin DT, Berry JA, Badger MR, Fock H, Osmond CB** (1980) Oxygen exchange in leaves in the light. Plant Physiol **66:** 302–307
9. **Chapin FS III, Bloom AJ, Field CB, Waring RH** (1987) Plant responses to multiple environmental factors. BioSci **37:** 49–57
10. **Elrifi IR, Turpin DH** (1986) Nitrate and ammonium induced photosynthetic suppression in N-limited *Selenastrum minutum*. Plant Physiol **81:** 273–279
11. **Fock H, Hilgenberg W, Egle K** (1972) Kohlendioxid- und sauerstoff-gaswechsel belichteter blatter und die $CO_2/O_2$-quotienten bei normalen und niedrigen $O_2$-partialdrucken. Planta **106:** 355–361
12. **Heusner AA, Tracy ML** (1984) Coulometric measurement of oxygen consumption in insects. *In* TJ Bradley, TA Miller, eds, Measurement of Ion Transport and Metabolic Rate in Insects. Springer-Verlag, Berlin, pp 163–186
13. **Kaplan A, Gale J, Poljakoff-Mayber A** (1976) Simultaneous measurement of oxygen, carbon dioxide, and water vapor exchange in intact plants. J Exp Bot **27:** 214–219
14. **Kaplan A, Björkman O** (1980) Ratio of $CO_2$ uptake to $O_2$ evolution during photosynthesis in higher plants. Z Planzenphysiol **96:** 185–188
15. **Kirschbaum MUF, Pearcy RW** (1988) Concurrent measurements of oxygen- and carbon-dioxide exchange during lightflecks in *Alocasia macrorrhiza* (L.) G. Don. Planta **174:** 527–533
16. **Luft KF, Mohrmann D** (1967) Neues Gerät zur paramagnetischen Sauerstoff-Messung. Chem-Ing-Techn **39:** 575–578
17. **McDermitt DK, Loomis RS** (1981) A new approach to the analysis of reductive and dissipative costs in nitrogen assimilation. *In* JM Lyons, RC Valentine, DA Phillips, DW Rains, RC Huffaker, eds, Genetic Engineering of Symbiotic Nitrogen Fixation and Conservation of Fixed Nitrogen. Plenum, New York, pp 639–650
18. **Myers J** (1949) The pattern of photosynthesis in *Chlorella*. *In* J Franck, WE Loomis, eds, Photosynthesis in Plants. Iowa State College Press, Cedar Falls, IA, pp 349–364
19. **Oaks A, Hirel B** (1985) Nitrogen metabolism in roots. Annu Rev Plant Physiol **36:** 345–365
20. **Pate JS** (1983) Patterns of nitrogen metabolism in higher plants and their ecological significance. *In* JA Lee, S McNeill, IH Rorison, eds, Nitrogen as an Ecological Factor. Blackwell Scientific Publ, Oxford, pp 225–255
21. **Robinson JM** (1986) Carbon dioxide and nitrite photoassimilatory processes do not intercompete for reducing equivalents in spinach and soybean leaf chloroplasts. Plant Physiol **80:** 676–684
22. **Robinson JM** (1988) Spinach leaf chloroplast $CO_2$ and $NO_2^-$ photoassimilations do not compete for photogenerated reductant. Manipulation of reductant levels by quantum flux density titrations. Plant Physiol **88:** 1373–1380
23. **Samish YB** (1978) Measurement and control of $CO_2$ concentration in air is influenced by the desiccant. Photosynthetica **12:** 73–75
24. **Schulze E-D, Bloom AJ** (1984) Relationship between mineral nitrogen influx and transpiration in radish and tomato. Plant Physiol **76:** 827–828
25. **Smirnoff N, Stewart GR** (1985) Nitrate assimilation and translocation by higher plants: comparative physiology and ecological consequences. Physiol Plant **64:** 133–140
26. **Volk RJ, Jackson WA** (1964) Mass spectrometric measurements of photosynthesis and respiration in leaves. Crop Sci **4:** 45–48
27. **Von Caemmerer S, Farquhar GD** (1981) Some relationships between the biochemistry of photosynthesis and the gas exchange of leaves. Planta **153:** 376–387
28. **Warner RL, Narayanan KR, Kleinhofs A** (1987) Inheritance and expression of NAD(P)H nitrate reductase in barley. Theor Appl Genet **74:** 714–717
29. **Weger HG, Turpin DH** (1989) Mitochondrial respiration can support $NO_3^-$ and $NO_2^-$ reduction during photosynthesis: interactions between photosynthesis, respiration, and N assimilation in the N-limited green alga *Selenastrum minutum*. Plant Physiol **89:** 409–415
30. **Weissbart J** (1975) S-3A Oxygen Analyzer—Operating and Service Manual. Applied Electrochemistry Inc, Sunnyvale, CA